Underwater Hovering Control with Fluidic Amplifiers

Fabio R. Goldschmied*
University of Utah, Salt Lake City, Utah

Hovering control of underwater vehicles requires both hydrostatic and hydrodynamic means. Fluidic amplifiers, particularly the axisymmetric focussed-jet design, are well suited for both control means because large flows can be switched on and off fast without water hammer in the pumps and piping system. A preliminary experimental investigation has been carried out with an axisymmetric amplifier at supply pressures up to 75 psig and flows up to 200 gal/min. Pressure recoveries over 50% and flow recoveries up to 150% have been measured. Thrust ratios over 80%, on the basis of propulsive jet thrust of equal fluid power, have been observed. Dynamic switching times have been measured from electric signal to thrust output; switching on requires 300 msec and off requires only 100 msec. On rise times are of the order of 100 msec while off decay times are less than 20 msec.

Nomenclature

P_s = diverter's supply pressure, lbf/in.^{2}
P_o = diverter's output pressure, lbf/in.^{2}
P_a = diverter's ambient (return) pressure, lbf/in.^{2}
P_c = diverter's control pressure, lbf/in.^{2}
Q_s = diverter's supply flow, ft^3/sec
Q_o = diverter's output flow, ft^3/sec
Q_c = diverter's control flow, ft^3/sec
C_{pc} = $(P_c - P_a)/(P_s - P_a)$ = Coanda suction coefficient
C_Q = $P_sD^4/\rho Qs^2$ = supply flow coefficient
D = diverter's supply inlet diameter, ft
A = cross-sectional area, ft
v = volume, ft^3
r = radius from center of rotation, ft
V = fluid velocity, fps
V_φ = tangential fluid velocity, fps
F = force summation, lbf
M = torque summation, ft/lbf
T = diverter's thrust, lbf
T_o = reference jet thrust, lbf
η = T/T_o = propulsive ratio of diverter
C_T = T/P_sD^2 = diverter's thrust coefficient
ρ = fluid mass density, lbfsec^2/ft^4
ν = fluid kinematic viscosity, ft^2/sec
cs = control surface for double integration, ft^2
cv = control volume for triple integration, ft^3

1. Introduction

HOVERING control of underwater vehicles requires both hydrostatic and hydrodynamic means. The first requires exact and timely shifting of ballast (water) among several buoyancy tanks. The latter exploits the dynamic effects of flow for the generation of precise thrust and torque pulses.

The generation of linear thrust by means of flow is governed by

$$F = \oiint_{cs} V(\rho V dA) + \frac{\partial}{\partial t}\iiint_{cv} V(\rho dv)$$

This equation relates the sum F of the force distribution to the rate of efflux of momentum across the control surface plus the time rate of change of momentum inside the control volume. Generally, only the first right-hand term has been exploited for generation of steady-state thrust. The potential usefulness of transient flow within the vehicle, the second right-hand term, has been neglected because of severe water-hammer effects.

Similarly, the generation of a rolling torque by means of flow is governed by

$$M = \iint_{cs} (rV\varphi)(\rho V dA) + \frac{\partial}{\partial t}\iiint_{cv} (rV\varphi)(\rho dv)$$

Again, the terms on the right-hand side represent the efflux of moment-of-momentum through the control surface plus the time rate of increase of moment-of-momentum inside the control volume, where both quantities are observed from the control volume. The well-known "fluid flywheel" exploits the second right-hand term and provides torque pulses without mass efflux.

Fluidic amplifiers offer a new underwater control technology with improved reliability and much faster response. The axisymmetric focussed-jet amplifier appears particularly suited. The pneumatic version of this amplifier is well known and has been described in popular survey articles[1,2] and technical books.[3,4] A general discussion comparing basic features of axisymmetric and planar amplifiers is given by Fox and Goldschmied,[5] including the first description of the focussed-jet axisymmetric monostable amplifier as invented and developed by the present author. The basic hydrodynamic principles of operation, the assembly design, and stainless steel fabrication are described by Goldschmied,[6] together with pneumatic digital control applications. Furthermore, dynamic testing methods for the amplifier in the NOR and NAND digital logic function have been proposed and presented by Goldschmied[7] together with preliminary experimental results. Input/output switching times of 0.5 and 0.25 msec have been documented by Goldschmied[6,8] at 5-psi pneumatic supply pressure as against 2 msec for a comparable Corning Glass Works planar NOR gate (catalog no. FD 2-4-3730).

All of the aforementioned effort[1–8] was directed to low-pressure (3–15 psi) pneumatic operation for digital NOR logic application with objectives of minimum size and weight, minimum fluid power requirements, and maximum switching speed; the major part of the engineering development was funded by NASA Marshall Space Flight Center† and is reported in Ref. 8. More recently, it has become apparent that large hydraulic diverters comprise a most important application for the axisymmetric amplifier since their use makes possible very fast switching of large liquid flows without concomitant upstream water-hammer pressure surges.

Presented as Paper 67-433 at the AIAA 3rd Propulsion Joint Specialist Conference, Washington, D.C., July 17–21, 1967; submitted September 25, 1967; revision received December 26, 1966.

* Director, Fluid Control Systems Laboratory, and Associated Research Professor of Mechanical Engineering. Member AIAA.

† Contracts NAS 8-11236 and NAS 8-20102 under the technical supervision of M. A. Kalange, Astrionics Laboratory.

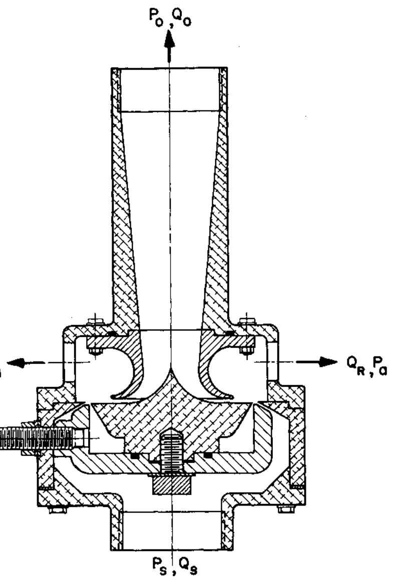

Fig. 1. Cross section of hydraulic axisymmetric focussed-jet diverter.

This paper presents a preliminary experimental investigation of the hydraulic amplifier, both as a flow diverter and as a thrust control device for potential underwater hovering control application.

2. Hydraulic Amplifier Development

The development of the large hydraulic axisymmetric diverter was based on the geometry of the small pneumatic amplifier given in Fig. 1.2.3.-1 of Ref. 8. Its size was arbitrarily increased fivefold, and a preliminary plexiglas model was built and tested by Karimi[9] at the University of Utah as a graduate thesis project. Even at low supply pressures of the order of 35 psi, a standing cavitation bubble was observed within the control body cavity, caused by the high suction of the annular power jet. A pneumatic pressure input was quite effective in providing fast and "clean" switching action. Another observation made during these preliminary tests was that a substantial transient thrust was obtained along the amplifier's axis with the on and off flow switching.

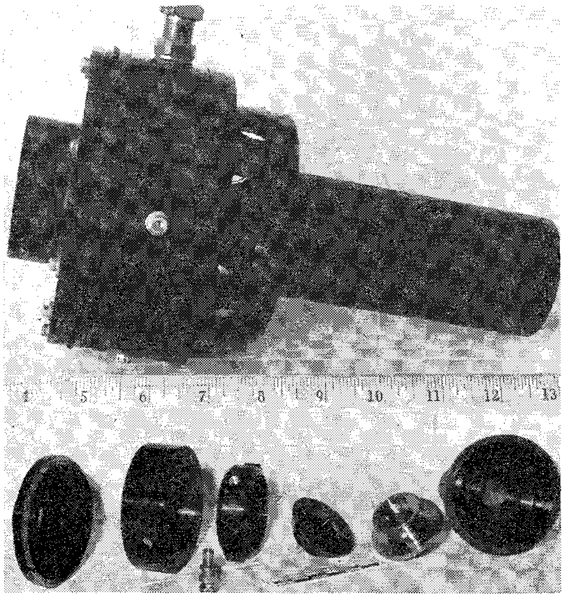

Fig. 2 Hydraulic axisymmetric diverter assembly (upper) and exploded view (lower).

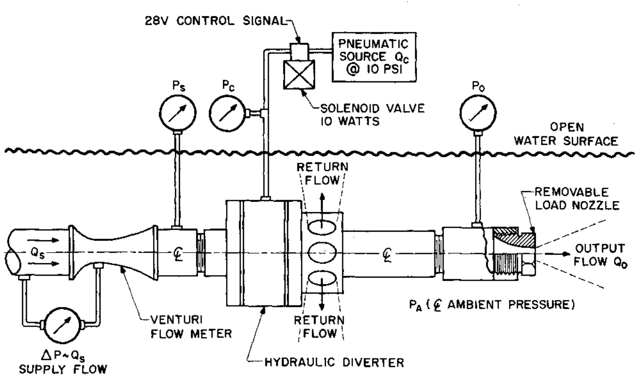

Fig. 3 Experimental test layout of hydraulic diverter in open flume.

Following this preliminary phase, a design study was carried out in the summer of 1966 at NASA's Marshall Space Flight Center‡ to produce an advanced version of the same hydraulic amplifier of minimum over-all size and weight and capable of withstanding over 200-psi supply pressure (see Goldschmied and Kalange[10]). Hard-anodized aluminum and stainless steel were employed in fabricating the amplifier. Its cross section is shown in Fig. 1. The maximum diameter is 6.00 in. and length is 11.00 in. Both the supply and the outlet diameters are 2.00 in. The six major parts identified in the cross-sectional layout can be fabricated on conventional machine tools. Figure 2 displays the diverter assembly (upper) and the exploded view (lower).

Flow Testing

Using the amplifier by NASA, a test program was carried out at the Hydraulic Laboratory of the University of Utah. The steady-state test arrangement is shown in Fig. 3. The amplifier is submerged in an open-channel flume which receives both the on axial discharge and the off radial flow return. The hydraulic steady-state performance is presented in Fig. 4 in terms of the dimensionless ratios P_o/P_s and Q_o/Q_s. It is seen that the output pressure is practically constant from blocked load to 90% supply flow. This is called the throttled-flow regime and it exploits a curved jet to maintain constant pressure regardless of flow rate. A sketch of the flow patterns is given in Fig. 5. After the 90% flow point, the jet is "swallowed" and cannot maintain its curvature. This is called the through-flow regime and it exhibits a fast pressure drop with increased flow (unlike the previous regime).

The Coanda attachment bubble must be considered in regard to its suction as a function of the output load. A good fluidic amplifier will be insensitive to load and the Coanda suction coefficient will be independent of load. Experimenta

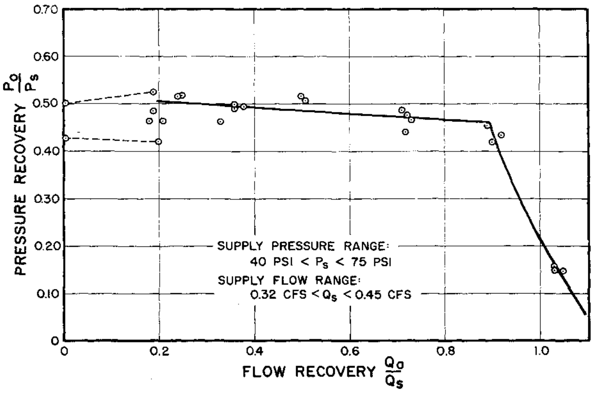

Fig. 4 Output performance of hydraulic diverter.

‡ ASEE/NASA Summer Faculty Fellowship.

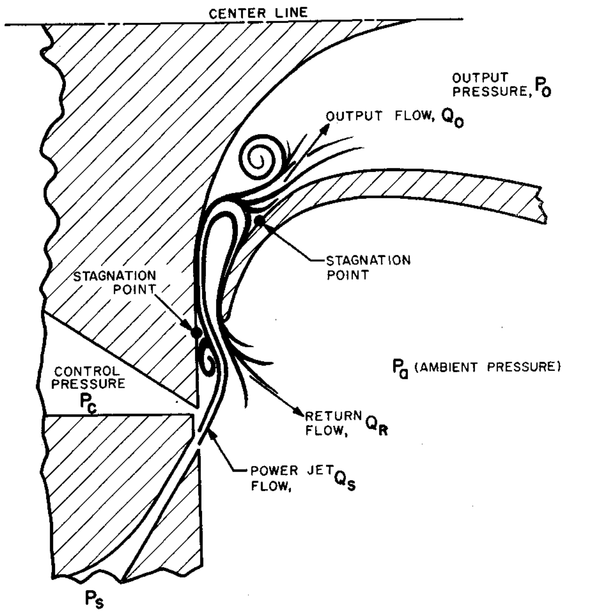

Fig. 5 Sketch of flow curvatures in throttled-flow regime.

data are given in Fig. 6, where C_{pc} (negative pressure) is plotted against the output flow ratio Q_o/Q_s. It is seen that, indeed, the Coanda suction is not affected by the output load and the amplifier is completely stable up to blocked load. The steady-state tests were carried out from 40 to 75 psi; similarity holds and there is no upstream water-hammer as switching is accomplished by pneumatic input of substantially atmospheric pressure (less than 10 psi) through a $\frac{1}{4}$-in.-diam line.

Thrust Testing

After the flow test phase, a thrust test program was carried out with the same amplifier in the open-channel flume. A hydraulic thrust-pendulum test stand for installation over the flume was designed and constructed. The complete assembly is shown in Fig. 7 with the flume empty. Water flow at up to 80 psi is introduced at the pendulum pivot point through a low-friction, 0-ring rotating joint. A Statham model UL-4 200-lbf load-cell was used with an analog readout model UR-5 and a dual-beam Tektronix oscilloscope. Control air is introduced via a 28-v, 10-w solenoid valve at the top of the test rig. The electric solenoid voltage is considered as system input and thrust as output.

Figure 8a shows the fluidic diverter installed and operating in the flow condition in the open-channel flume. The trace of the axial output jet is clearly visible. Figure 8b displays the diverter in the fully off flow condition with all the flow exiting radially and no axial output.

It has been seen in Fig. 4 that a substantial pressure loss is encountered in going through the diverter, i.e., the pressure recovery is about 50%. By the same token, the diverter's thrust will be less than that of a propulsive nozzle sized to accept the same supply flow Q_s at the given supply pressure P_s; the criterion of comparison is chosen to be the fluid supply power P_sQ_s available for generation of thrust either through the fluidic diverter or through the conventional valve and nozzle.

Figure 9 shows supply pressure P_s plotted against the supply flow Q_s for the diverter and for a nozzle of 0.875-in.-diam. This nozzle was one of the set employed to effect the output load on the diverter. The two curves (diverter and propulsive jet) are equivalent with regard to flow, pressure, and, therefore, fluid power demand.

In Fig. 10, thrust is plotted against supply pressure for several propulsive jets (nozzle diameters 1.415, 1.218, 1.00, 0.875, and 0.710 in.) and for the amplifier with three output load nozzles (1.00, 1.218, and 1.415 in.). The nozzles are the same, whether employed directly for the propulsive jet or installed as a load device on the amplifier.

The thrust comparison at equal fluid supply power is made between the 0.875-in. nozzle line and the 1.218-in. diverter line (maximum thrust). A substantial thrust loss can be observed between the two. As a matter of interest, the maximum diverter thrust line agrees well with the 0.710-in. propulsive nozzle line.

The propulsive ratio of the diverter is defined as the ratio of its thrust to that of the 0.875-in. nozzle at the same supply pressure and, therefore, at the same supply power. This ratio is a function of the amplifier output load or output flow ratio Q_o/Q_s and is affected by the supply pressure, as seen in Fig. 11. The peak occurs at $Q_o/Q_s = 1.0$ with an output nozzle of 1.218-in.-diam.

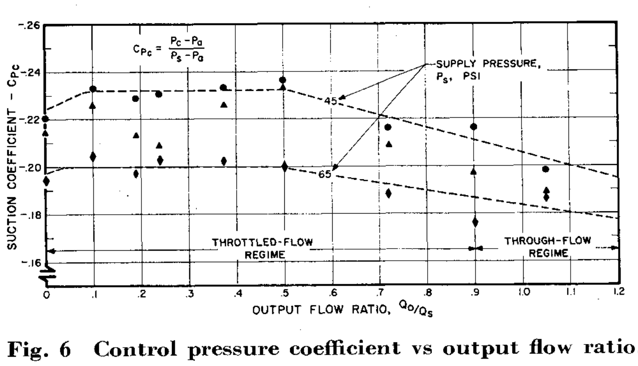

Fig. 6 Control pressure coefficient vs output flow ratio.

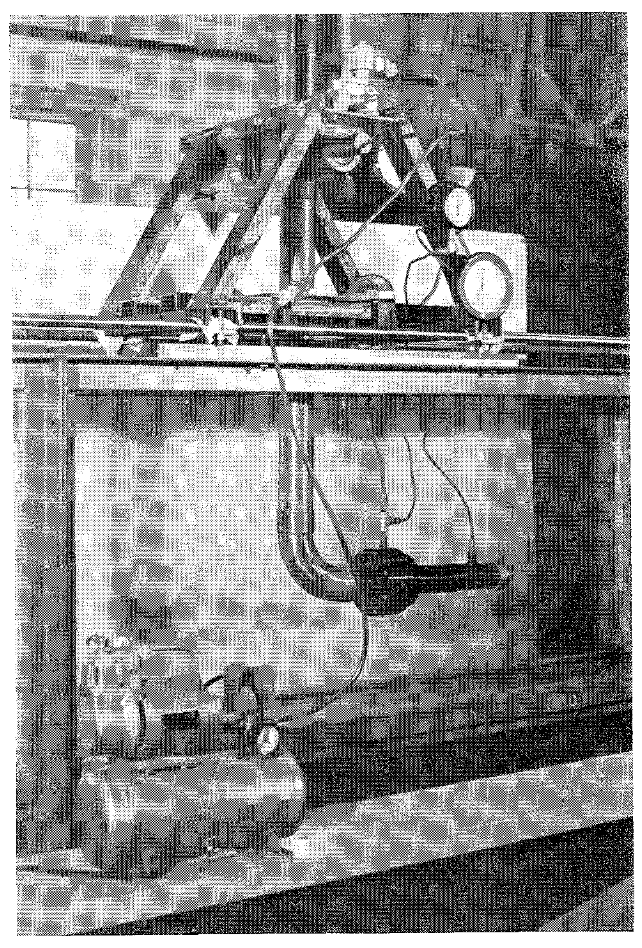

Fig. 7 Thrust test stand with fluidic thruster in empty flume.

The diverter must operate submerged and, therefore, all thrust measurements comprised a submerged output jet. For the propulsive jet data, on the other hand, measurements were taken with the liquid jet submerged both in water and in air. The same thrust was measured in both cases for a given pressure differential across the nozzle.

The ideal one-dimensional momentum thrust has been computed for the propulsive nozzles from measured flow rate and measured nozzle area, assuming uniform nozzle velocity. The experimental thrust data are approximately 60% of the ideal values.

If an estimate is to be made of the actual diverter thrust extrapolated to large sizes and deep submergence, then it should be increased to match the theoretical momentum thrust. This would not alter Fig. 11, since only thrust ratios are presented.

Dynamic Switching Tests

The principal characteristic of fluidic amplifiers, such as the present axisymmetric device, is the ability to switch flow on and off rapidly without moving or deforming mechanical parts. This dynamic switching was investigated following the steady-state thrust tests with respect to input/output switching times, thrust rise times, and decay times.

The input instant is taken as the initial signal from the 28-v, 10-w activation circuit for the solenoid valve controlling the pneumatic input to the amplifier. Output is taken as the thrust itself. Input/output time is defined from the electrical step (zero rise time for this purpose to 90 or 10% full thrust). In case there is a transient force during the switching, then the 90 or 10% applies to the transient peak. The thrust rise time is defined from 10 to 90% of the peak force. Similarly the decay time is defined from 90 to 10% of the peak force.

Figure 12 shows a typical switching time pattern for the tests. The upper trace is the output thrust signal and the lower trace is input electrical signal. The switching is commanded manually at 0.5 cps. The supply pressure is 60 psi and the load on the amplifier is provided by an output nozzle diameter of 1.415 in. Although this nozzle gives less than maximum thrust, as seen in Figs. 10 and 11, the switching phenomenon is considered more difficult at the higher flows and, therefore, the test is more severe.

Figure 12 shows one cycle in greater time detail at the same pressure and load. The off input/output time appears to be

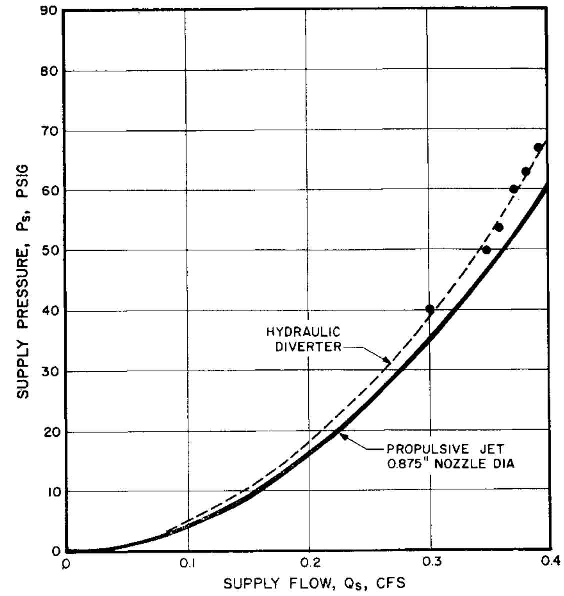

Fig. 9 Supply presssure and flow of hydraulic diverter and of propulsive jet.

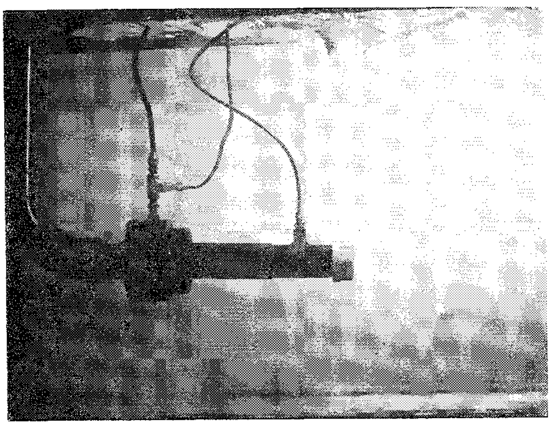

a) "On" flow condition

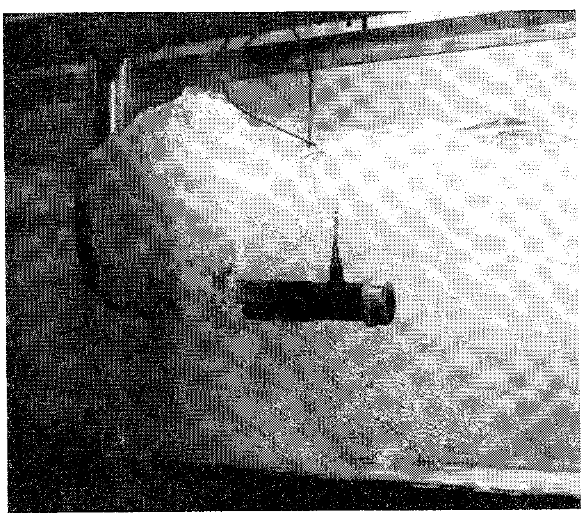

b) "Off" flow condition

Fig. 8 Fluidic Thruster in hydraulic flume at 75-psi supply pressure.

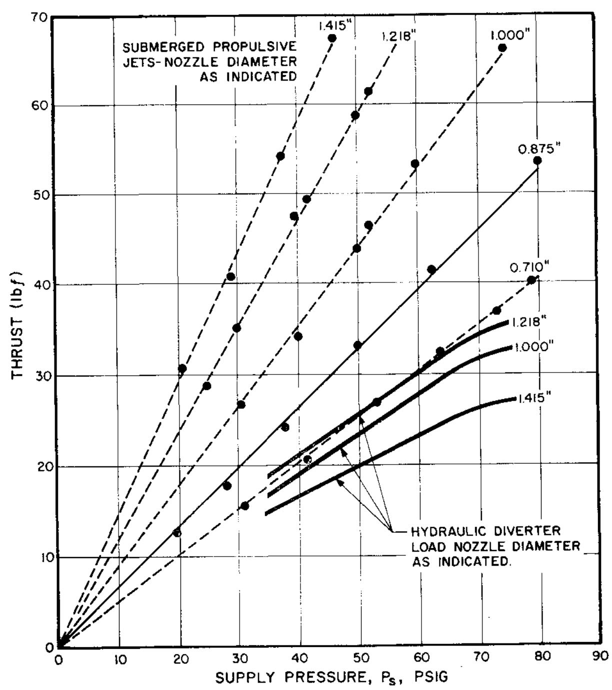

Fig. 10 Steady-state thrust map for hydraulic diverter and for propulsive jets.

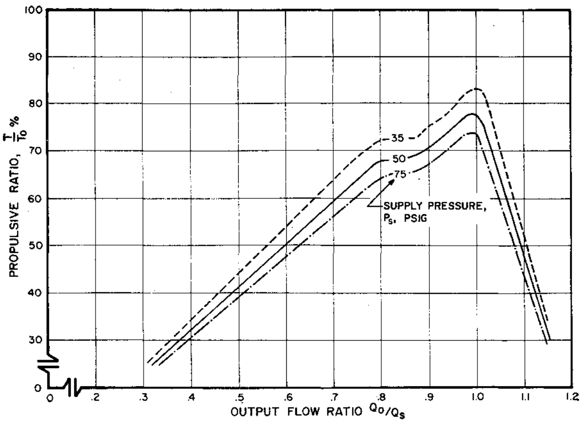

Fig. 11 **Steady-state propulsive ratio of hydraulic diverter vs output flow ratio.**

100 msec while the on input/output time is much longer, of the order of 300 msec. The on rise time is less than 100 msec while the off decay time is extremely fast, less than 20 msec.

3. Hovering Control Applications

Hovering control of hydrospace vehicles is important in many applications. It can be accomplished by modification of the mass distribution of the hydrospace vehicle (i.e., by pumping water from one buoyancy tank to another) and it also can be achieved by dynamic means involving fluid mass ejection and transient flow within the vehicle.

Hydrostatic Control

The axisymmetric amplifier is well-suited to provide hydrostatic hovering control because it can start and stop large liquid flows very fast, reliably (no moving parts), and without upstream water-hammer.

For system engineering, the following information is required: 1) geometry of the amplifier (see Fig. 1); 2) supply flow requirements (see Fig. 9) and flow coefficient, $C_Q = P_s D^4/\rho Q_s^2 = 0.00121$; 3) steady-state hydraulic output performance (see Fig. 4); 4) switching times, both on and off (see Fig. 12); and 5) typical tank installation, as shown in Fig. 13. The minimum operating supply pressure P_s has been found to be about 30 psi. A maximum has not been determined, as yet, beyond the 75-psi level.

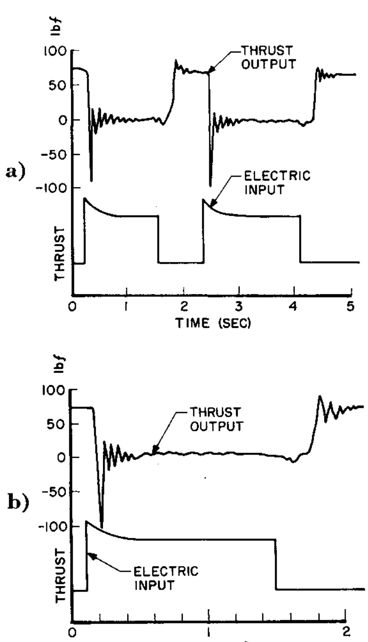

Fig. 12 **Dynamic thrust of hydraulic diverter (P_s = 60 psi, 1.415-in. nozzle diam).**

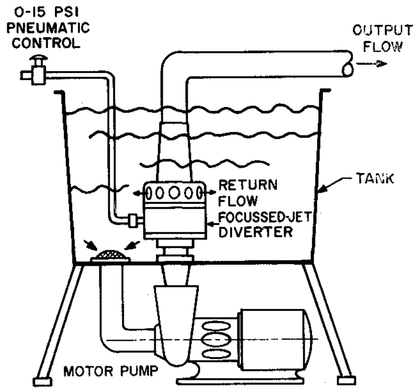

Fig. 13 Typical tank installation of hydraulic diverter with pneumatic control.

Hydrodynamic Control

Hydrodynamic controls may be classified into steady-state, mass-ejection devices that produce steady thrust, and transient-flow, nonejecting devices that produce thrust pulses.

Mass ejection devices

For the first category, the axisymmetric amplifier as a thrust control device may be modified, compared to the flow-control version, by eliminating the diffuser section. The final version of such a device is shown in Fig. 14. Its over-all dimensions are only $5\frac{1}{4}$-in. length and 6-in. diam with the inlet still 2-in. National Pipe Thread (NPT) and the outlet reduced to 1.218-in. diameter. The engineering information required is as follows:

1) Thrust coefficient $C_T{}^* = T^*/P_s D^2 = 0.212$. The thrust T^* is the optimum test value extrapolated to larger nozzles (Reynolds numbers) and deep submergence (see Sec. 2 "Thrust Testing"). The characteristic length D is the inlet diameter where the supply flow enters.

2) Supply flow coefficient $C_Q = P_s D^4/\rho Q_s^2 = 0.00121$. Note that Q_s is not affected by switching amplifier on or off.

3) Propulsive ratio η for thrust T_o of a nozzle with upstream butterfly valve set to require equal flow rate at the given pressure (see Fig. 11); $\eta = T/T_o \simeq 0.80$

4) Over-all geometry (see Fig. 14).

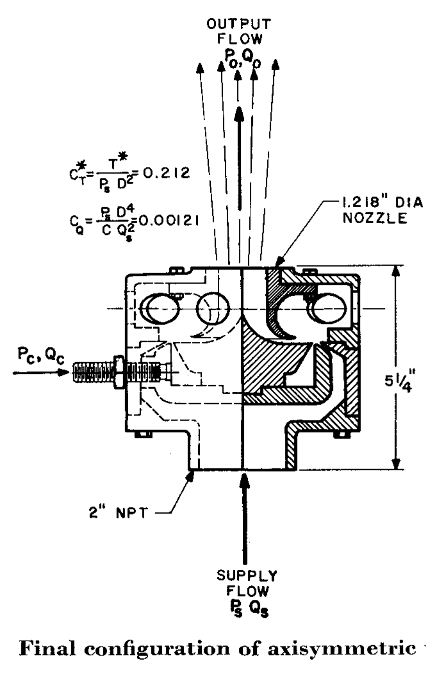

Fig. 14 **Final configuration of axisymmetric thruster.**

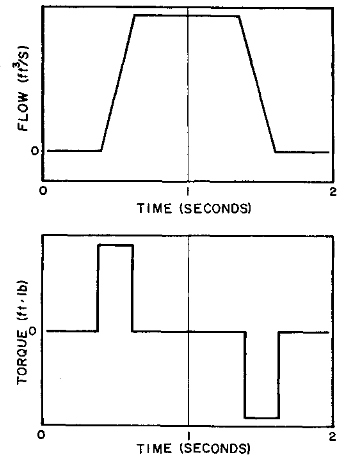

Fig. 15 Ideal flow and torque of fluid flywheel.

Nonejecting devices

For the second category, the fluid flywheel is the best known application for roll control of an aerospace or hydrospace vehicle. It produces torque pulses as the flow within a closed fluid loop is accelerated or decelerated. Figure 15 is an idealized picture of flow and torque vs time. A demonstration of a fluidic flywheel is reported by Goldschmied and Kalange[10] for a pulsatile fluidic heart pump described by Goldschmied, Prakouras, and Nelson.[11] Figure 16 shows a 50-in.-diam double loop of 0.75-in.-diam Tygon tubing connected with the centrally located heart pump. The entire assembly and the supporting turntable (350-lbf weight) were mounted on a high-grade, rotating air-bearing operating at 85-psi air pressure. Thus, a very high ratio of inertia to friction was achieved, simulating the rolling motion of a vehicle in space.

The heart pump (driven by a fluidic flip-flop operating with compressed air) produces fairly sharp flow pulses vs time, as shown idealized in Fig. 15. Correspondingly, there will be a torque pulse (positive or negative) for the flow rise or decay. The positive torque pulse would start a vehicle into angular motion. After a time increment, the negative torque pulse stops the motion. After a complete cycle, no net energy is gained but an angular displacement is achieved.

Operating the heart pump at about 35-psi supply pressure resulted in a displacement of about 2° per flow pulse. The same effect can be achieved on a far larger scale using a conventional steady-state centrifugal pump and the axisymmetric amplifier to turn the flow on or off as desired.

4. Conclusions

The hydraulic version of the axisymmetric focussed-jet fluidic amplifier is applicable to underwater hovering control through 1) hydrostatic buoyancy control, 2) hydrodynamic linear thrust control, and 3) fluid flywheel roll control. The hydraulic pressure recovery is over 50% and the propulsive ratio over 80%. Switching is quite fast, of the order of 0.10 sec, and without upstream water-hammer effects.

To pinpoint specifications of actual hovering control devices, a preliminary design effort is needed. This can be done using information in this paper, together with the analysis of Strumpf[12] of the hovering response in an ocean current of a streamlined hull with stern propeller, bow and stern thrusters, mercury fluid flywheel, and tail empennage.

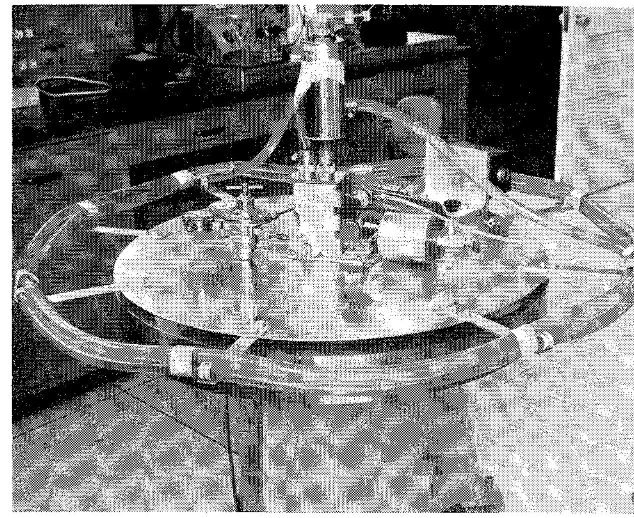

Fig. 16 Fluid flywheel roll-control demonstration.

References

[1] Wood, O. L., "Pure Fluid Devices," *Machine Design*, June 24, 1965.

[2] Letham, D. L., "Fluidic System Design," *Machine Design*, Feb. 17, 1966.

[3] Kirshner, J. M., *Fluid Amplifiers*, McGraw-Hill, New York, 1966, pp. 238–239.

[4] Humphrey, E. H. and Tarumato, D. H., eds., *Fluidics*, Fluid Amplifier Associates, Boston, 1965, pp. 24–25.

[5] Fox, H. L. and Goldschmied, F. R., "Basic Requirements for an Analytical Approach to Pure Fluid Control Systems," *Proceedings of the Second Fluid Amplification Symposium*, Vol. 1, Harry Diamond Labs., Washington, D.C., May 1964, pp. 293–300.

[6] Goldschmied, F. R., "Fluid Digital Amplifiers of Axisymmetric Focussed-Jet Design," *Fluidics*, edited by E. F. Humphrey and D. H. Tarumato, Fluid Amplifier Associates, Boston, 1965, pp. 215–221.

[7] Goldschmied, F. R., "Proposed Test Standards for NOR and NAND Fluid Digital Amplifiers with some Preliminary Experimental Results," *Proceedings of the 1965 Joint Automatic Control Conference*, American Society of Mechanical Engineers, Troy, New York, June 1965, pp. 150–153.

[8] Goldschmied, F. R. et al., "Analytical Investigation of Fluid Amplifiers' Dynamic Characteristics," CR-244 and CR-245, July 1965, NASA.

[9] Karimi, M., "Experimental Investigation of a Hydraulic Focussed-Jet Diverter with Pneumatic Control," unpublished M.S. thesis, June 1966, University of Utah.

[10] Goldschmied, F. R. and Kalange, M. A., "Hydraulic Axisymmetric Focussed-Jet Diverters with Pneumatic Control," TM X-53554, Dec. 15, 1966, NASA.

[11] Goldschmied, F. R., Prakouras, A. G., and Nelson, R. M., "Experimental Investigation of Fluidic and Peristaltic Heart Pumps," Paper 66-929, 1966, AIAA.

[12] Strumpf, A., "Cruising and Hovering Response of a Tail-Stabilized Submersible," *Journal of Hydronautics*, Vol. 1, No. 2, Oct. 1967, pp. 89–96.